Dynamic Coordination of Multiple Vessels for Offshore Platform Transportation

Du, Zhe; Negenborn, Rudy R.; Reppa, Vasso

DOI
10.1109/CCTA49430.2022.9965992

Publication date
2022

Document Version
Final published version

Published in
Proceedings 2022 IEEE Conference on Control Technology and Applications, CCTA 2022

2022 IEEE Conference on Control Technology and Applications (CCTA)
August 22-25, 2022. Trieste, Italy

Dynamic Coordination of Multiple Vessels for Offshore Platform Transportation

Zhe Du, Rudy R. Negenborn, Vasso Reppa

Abstract— **This paper proposes a novel dynamic coordination control scheme for a physically connected multi-vessel towing system to transport an offshore platform. The transportation process is executed by four tugboats, and each of them has a leading or following role. To render the transportation faster, the roles of the tugboats can be switched in the towing process. The dynamic coordination decision mechanism is designed to allocate in real-time a combination of roles to the tugs by comparing the position and heading of the offshore platform to the next waypoint position. A control allocation strategy is developed to optimally control the position and heading of the tugboats considering multiple constraints. The reference trajectory of the tugboats is dynamically calculated based on the assigned role of each tugboat. A simulation experiment indicates that the proposed control scheme can enhance the maneuverability of the physically connected multi-vessel towing system and increase the efficiency of offshore platform transportation.**

2022 IEEE Conference on Control Technology and Applications (CCTA) | 978-1-6654-7338-5/22/$31.00 ©2022 IEEE | DOI: 10.1109/CCTA49430.2022.9965992

I. INTRODUCTION

The requirements of ocean renewable energy (wind and wave energy) motivate the increase of establishing offshore platforms [1]. Transporting a huge floating object from inland waters to the open sea is an important but also hazardous mission. Usually, an offshore platform is manipulated by coordinating several physical-connected tugboats. In recent decades, the rapid development of autonomous surface vessels (ASVs) has enabled multi-vessel system missions in more complex maritime operations [2]. Floating object transportation is one of the typical applications.

Research on the floating object transportation by multiple ASVs can be classified into two categories: attached manipulation and tow-based manipulation. The first category is based on the idea of object manipulation by multi-robot systems [3]. In this case, each ASV attaches to the surface of the object tightly, treated as an actuator. In research work [4], six ASVs attach to a distressed ship, the control strategy is based on optimal and adaptive control combining Lyapunov theory. In [5], authors use the redistributed pseudo-inverse algorithm, which is based on an optimization method and adaptive sliding mode control method to achieve a task of ship berthing by four ASVs. Authors in [6] propose a distributed model predictive control method for three ASVs to cooperatively transport a floating object, where two ASVs symmetrically and tightly connect to the two sides of an object, and one ASV attaches at the back of the object.

The second category adopts the common practice in maritime: towing manipulation, which is more suitable for dynamic offshore water surface environments. In this case, each ASV is connected to the object by a towline. Scholars in [7] focus on the course-keeping control of a cylindrical drilling platform towing system by designing a reinforcement learning-based control method. In [8], an extended backstepping control method is proposed to let two ASVs cooperate to manipulate a large buoyant load tracking a desired trajectory. In [9], a distributed robust cooperative trajectory tracking control scheme is devised for a towing system with four ASVs based on the dynamic surface control technique, adaptive law, and graph theory. The common practice of the towing-based manipulation methods (also for ships [10]–[12]) is to consider that the tugboats have a fixed role. However, this restrains the maneuverability of the towing system and delays transportation.

The goal and main contribution of this work is the design of a control scheme to dynamically coordinate multiple tugboats by alternating their roles in the transportation of an offshore platform. The problem is formulated in Section 2. The steps of the dynamic coordination given in Section 3 are: first, allocate a combination of roles to the tugs according to the relations between the position and heading of the platform and the next waypoint; then, calculate the reference trajectory of the tugboats based on the assigned roles of each tug; finally, compute the control inputs for tugboats to track their reference trajectories considering multiple constraints. In Section 4, simulation experiments are carried out to illustrate the potential of the proposed method. Conclusions and future research directions are given in Section 5.

II. PROBLEM STATEMENT

This work aims to efficiently transport an offshore platform to the desired position using four autonomous tugboats. The motion of the platform and tugboats is described by the 3-DoF (degree of freedom) hydrodynamic model [13], where the kinematics and kinetics are expressed as:

$$\begin{aligned} &\dot{\boldsymbol{\eta}}_*(t) = \boldsymbol{R}\big(\psi_*(t)\big)\boldsymbol{\nu}_*(t) \\ &\boldsymbol{M}_*\dot{\boldsymbol{\nu}}_*(t) + \boldsymbol{C}_*\big(\boldsymbol{\nu}_*(t)\big)\boldsymbol{\nu}_*(t) + \boldsymbol{D}_*\boldsymbol{\nu}_*(t) = \boldsymbol{\tau}_*(t), \end{aligned} \tag{1}$$

where $*$ stands for O (offshore platform) or I (tugboat, $I \in \{\mathrm{A},\mathrm{B},\mathrm{C},\mathrm{D}\}$); $\boldsymbol{\eta}_*(t) = [x_*(t)\ \ y_*(t)\ \ \psi_*(t)]^{\mathrm{T}} \in \mathbb{R}^3$ is the position vector in the world frame (North-East-Down) including position coordinates $\big(x_*(t),\ y_*(t)\big)$ and heading $\psi_*(t)$; $\boldsymbol{\nu}_*(t) = [u_*(t)\ v_*(t)\ r_*(t)]^{\mathrm{T}} \in \mathbb{R}^3$ is the velocity vector in the body-fixed frame containing the velocity of surge $u_*(t)$, sway $v_*(t)$ and yaw $r_*(t)$; $\boldsymbol{R} \in \mathbb{R}^{3\times3}$ is the rotation matrix from the body frame to the world frame, which is a function of heading; $\boldsymbol{M}_* \in \mathbb{R}^{3\times3}$, $\boldsymbol{C}_* \in \mathbb{R}^{3\times3}$ and $\boldsymbol{D}_* \in$

Zhe Du, Rudy R. Negenborn, and Vasso Reppa are with the Department of Maritime and Transport Technology, Delft University of Technology, 2628 CD Delft, The Netherlands (e-mail: Z.Du@tudelft.nl; R.R.Negenborn@tudelft.nl; V.Reppa@tudelft.nl).

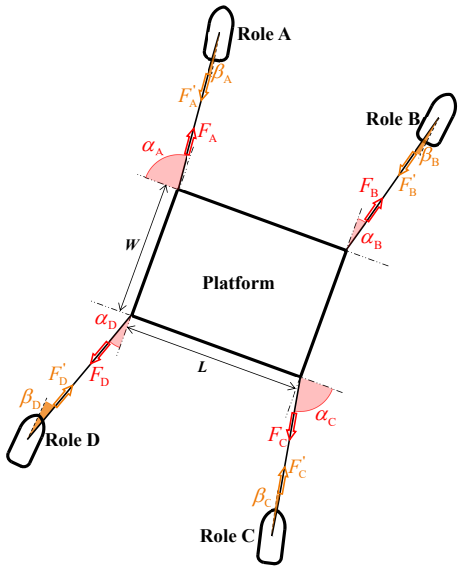

Fig. 1: Schematic diagram of force for the towing system.

$\mathbb{R}^{3\times3}$ are the mass (inertia), Coriolis-Centripetal and damping matrices, respectively; $\boldsymbol{\tau}_*(t) = [\tau_{*\mathrm{u}}(t)\ \tau_{*\mathrm{v}}(t)\ \tau_{*\mathrm{r}}(t)]^{\mathrm{T}} \in \mathbb{R}^3$ is the controllable input referring to the forces $\tau_{*\mathrm{u}}(t)$, $\tau_{*\mathrm{v}}(t)$ and moment $\tau_{*\mathrm{r}}(t)$ in the body-fixed frame. Fig. 1 is the schematic diagram showing the forces on the towing system. The controllable inputs of the platform denoted by $\boldsymbol{\tau}_O(t)$ are the forces from the towlines applied by four tugs. We define two roles for these tugs: Role A and B are leading tugs, whose role is to accelerate the speed and adjust the heading of the platform; Role C and D are following tugs, whose role is to slow down the speed and stabilize the heading of the platform. Thus, $\boldsymbol{\tau}_O(t)$ is expressed as:

$$\begin{aligned}\boldsymbol{\tau}_O(t) &= \boldsymbol{\tau}_{O_\mathrm{A}}(t) + \boldsymbol{\tau}_{O_\mathrm{B}}(t) + \boldsymbol{\tau}_{O_\mathrm{C}}(t) + \boldsymbol{\tau}_{O_\mathrm{D}}(t) \\ &= \boldsymbol{B}_{O_\mathrm{A}}\big(\alpha_\mathrm{A}(t)\big)F_\mathrm{A}(t) + \boldsymbol{B}_{O_\mathrm{B}}\big(\alpha_\mathrm{B}(t)\big)F_\mathrm{B}(t) + \\ &\quad \boldsymbol{B}_{O_\mathrm{C}}\big(\alpha_\mathrm{C}(t)\big)F_\mathrm{C}(t) + \boldsymbol{B}_{O_\mathrm{D}}\big(\alpha_\mathrm{D}(t)\big)F_\mathrm{D}(t),\end{aligned} \tag{2}$$

where $F_\mathrm{A}(t) \sim F_\mathrm{D}(t)$ are the towing forces, $\alpha_\mathrm{A}(t) \sim \alpha_\mathrm{D}(t)$ are the towing angles, which can be seen in Fig. 1; $\boldsymbol{B}_{O_\mathrm{A}} \sim \boldsymbol{B}_{O_\mathrm{D}} \in \mathbb{R}^3$ are the platform configuration matrices, which are the function of towing angles:

$$\boldsymbol{B}_{O_\mathrm{A}} = \begin{bmatrix} \sin(\alpha_\mathrm{A}(t)) \\ -\cos(\alpha_\mathrm{A}(t)) \\ 0.5L\sin(\alpha_\mathrm{A}(t)) - 0.5W\cos(\alpha_\mathrm{A}(t)) \end{bmatrix} \tag{3}$$

$$\boldsymbol{B}_{O_\mathrm{B}} = \begin{bmatrix} \cos(\alpha_\mathrm{B}(t)) \\ \sin(\alpha_\mathrm{B}(t)) \\ 0.5W\sin(\alpha_\mathrm{B}(t)) - 0.5L\cos(\alpha_\mathrm{B}(t)) \end{bmatrix}, \tag{4}$$

$$\boldsymbol{B}_{O_\mathrm{C}} = \begin{bmatrix} -\sin(\alpha_\mathrm{C}(t)) \\ \cos(\alpha_\mathrm{C}(t)) \\ 0.5L\sin(\alpha_\mathrm{C}(t)) - 0.5W\cos(\alpha_\mathrm{C}(t)) \end{bmatrix}, \tag{5}$$

$$\boldsymbol{B}_{O_\mathrm{D}} = \begin{bmatrix} -\cos(\alpha_\mathrm{D}(t)) \\ -\sin(\alpha_\mathrm{D}(t)) \\ 0.5W\sin(\alpha_\mathrm{D}(t)) - 0.5L\cos(\alpha_\mathrm{D}(t)) \end{bmatrix}, \tag{6}$$

where L and W are the length and width of the platform.

The controllable inputs of the tugboats denoted by $\boldsymbol{\tau}_I(t)$ are the thruster forces and moment (omnidirectional forces generated by azimuth thrusters [14]). For tug A and B, the effects from the towing lines are the drag forces, their controllable inputs are expressed as:

$$\boldsymbol{\tau}_I(t) = \boldsymbol{\tau}_{T_I}(t) - \boldsymbol{B}_T\big(\beta_I(t)\big)F_I^{'}(t) \qquad (I = \mathrm{A},\mathrm{B}); \tag{7}$$

for tug C and D, the effects from the towing lines are the propulsive forces, their controllable inputs are expressed as:

$$\boldsymbol{\tau}_I(t) = \boldsymbol{\tau}_{T_I}(t) + \boldsymbol{B}_T\big(\beta_I(t)\big)F_I^{'}(t) \qquad (I = \mathrm{C},\mathrm{D}), \tag{8}$$

where $\boldsymbol{\tau}_{T_I}(t) \in \mathbb{R}^3$ are the thruster forces and moment of the tug I; $F_I^{'}(t)$ is the force applied through a controlled winch onboard the tugboat to the towing line. Assuming no force loss on the towing line, then $F_I^{'}(t) \equiv F_I(t)$. The winch onboard can control the length of the towline to enable it tight. Since the scope of this work focuses on the high-level control, the low-level winch control is not considered.

The term $\boldsymbol{B}_T \in \mathbb{R}^3$ is the tug configuration matrix, which is a function of the tug angle $\beta_I(t)$ (shown in Fig. 1):

$$\boldsymbol{B}_T = \begin{bmatrix} \cos\big(\beta_I(t)\big) \\ \sin\big(\beta_I(t)\big) \\ 0 \end{bmatrix} \qquad (I = \mathrm{A},\mathrm{B},\mathrm{C},\mathrm{D}). \tag{9}$$

III. DYNAMIC COORDINATION CONTROL

The control diagram is shown in Fig. 2. The dynamic coordination decision system determines the role of each tugboat $g(i,t)$ according to the coordinates of the current waypoint j $(x_{\mathrm{wp}}(j), y_{\mathrm{wp}}(j))$ and the current position vector of the platform $\boldsymbol{\eta}_O(t)$, where $g(i,t), (i \in \{1,2,3,4\})$ is a tag function for tugboats to distinguish the roles A, B, C, D. The control allocation system uses the above calculated data and the information of the current position and velocity from the four tugboats and the platform to compute the thruster forces and moment for each tugboats $\boldsymbol{\tau}_{T_i}(t)$. Finally, each tugboat provides the towing forces and moment $\boldsymbol{\tau}_{O_i}(t)$ to the offshore platform system for executing the transportation mission.

A. Dynamic Coordination Decision Mechanism

The mechanism of the dynamic coordination decision is based on the relative position between the platform and the current waypoint. As shown in Fig. 3, when the angle θ_O from the heading of the platform to the direction of the current waypoint is within a certain value and the waypoint is at the front of the platform, (Fig. 3 (a)), the front tugboats ① and ② are assigned as the leading tugs (Role A and B), the behind tugboats ③ and ④ are assigned as the following tugs (Role C and D); when the angle θ_O is over the certain value and the waypoint is at the direction of the right side of the platform (Fig. 3 (b)), the right-side tugboats ② and ③ are appointed as the leading tugs (Role A and B), the left-side tugboats ④ and ① are appointed as the following tugs (Role C and D).

The calculation of the angle from the heading of the

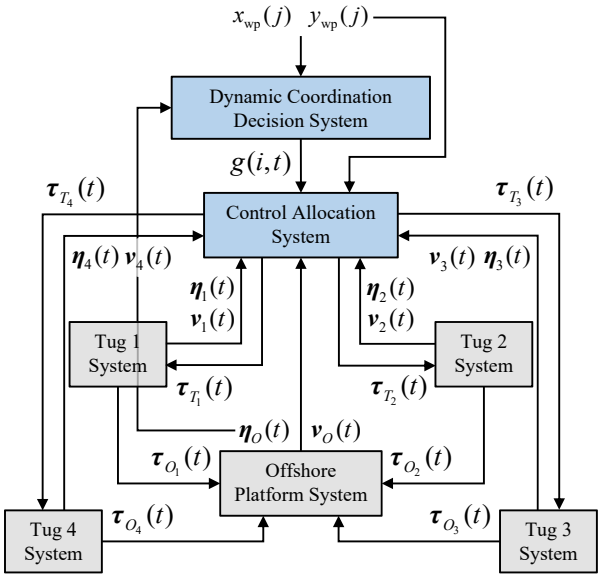

Fig. 2: Control diagram of the dynamic coordination of four tugboats to transport an offshore platform.

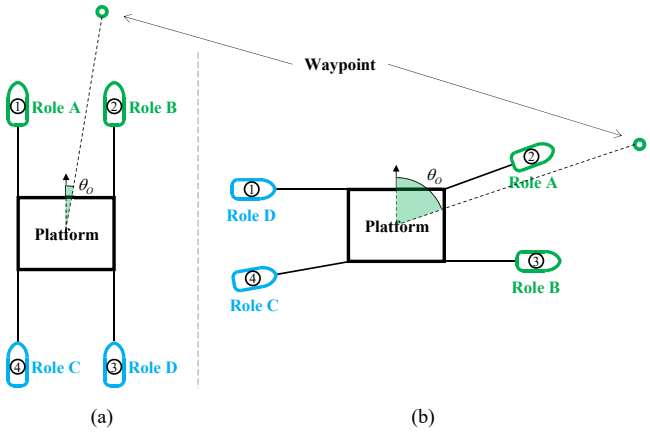

Fig. 3: Alternating roles between tugboats.

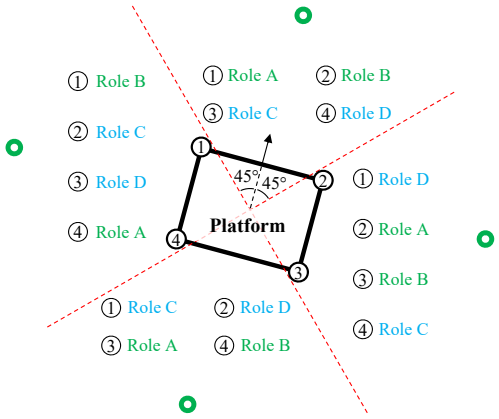

Fig. 4: Four role combinations of the tugboats. The number within the circle indicates the tugboat with an assigned role (A, B, C or D). The green circle stands for the waypoint.

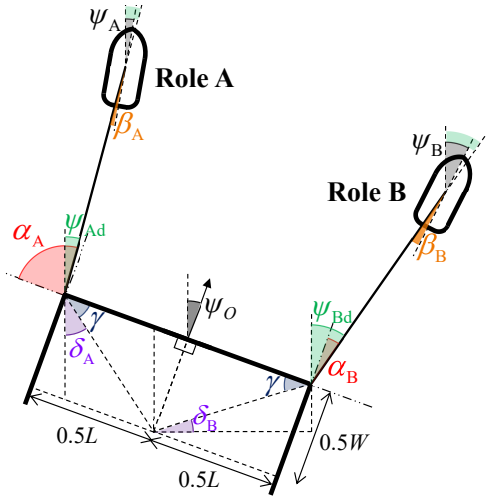

Fig. 5: Desired geometrical configuration of the system.

platform to the direction of the waypoint is expressed as:

$$\theta_O(t) = \arctan\left(\frac{x_{\text{wp}}(j) - x_O(t)}{y_{\text{wp}}(j) - y_O(t)}\right) - \psi_O(t), \tag{10}$$

where $(x_O(t), y_O(t))$ are the coordinates of the platform. There are four role combinations according to the angle θ_O, and the range for each combination is 90°. The different role combinations are shown in Fig. 4.

Each role corresponds to a specific reference trajectory of the tugboat, which is calculated through the desired kinematics configuration of the towing system. For the leading roles A and B (as shown in Fig. 5), the key to coupling the motion of the platform and the tugboats are the following angles:

$$\begin{aligned} \gamma &= \arctan\left(\tfrac{W}{L}\right) \\ \delta_{\text{A}}(t) &= 90^\circ - \gamma - \psi_O(t) \\ \delta_{\text{B}}(t) &= \gamma - \psi_O(t), \end{aligned} \tag{11}$$

where γ is the platform configuration angle; $\delta_{\text{A}}(t)$ and $\delta_{\text{B}}(t)$ are the linking angles of role A and B. The reference position and heading of the tugboats then are expressed as:

$$\begin{aligned} \psi_{\text{Ad}}(t) &= \alpha_{\text{A}}(t) + \psi_O(t) - 90^\circ \\ x_{\text{Ad}}(t) &= x_O(t) + L_O \cos\left(\delta_{\text{A}}(t)\right) + L_{\text{tow}} \cos\left(\psi_{\text{Ad}}(t)\right) \\ y_{\text{Ad}}(t) &= y_O(t) - L_O \sin\left(\delta_{\text{A}}(t)\right) + L_{\text{tow}} \sin\left(\psi_{\text{Ad}}(t)\right), \end{aligned} \tag{12}$$

$$\begin{aligned} \psi_{\text{Bd}}(t) &= \alpha_{\text{B}}(t) + \psi_O(t) \\ x_{\text{Bd}}(t) &= x_O(t) - L_O \sin\left(\delta_{\text{B}}(t)\right) + L_{\text{tow}} \cos\left(\psi_{\text{Bd}}(t)\right) \\ y_{\text{Bd}}(t) &= y_O(t) + L_O \cos\left(\delta_{\text{B}}(t)\right) + L_{\text{tow}} \sin\left(\psi_{\text{Bd}}(t)\right), \end{aligned} \tag{13}$$

where L_{tow} is the desired length of the towline (all the towlines are assumed the same value); L_O is the distance from the centre of gravity of the platform to its towing point, calculated by:

$$L_O = \sqrt{(0.5L)^2 + (0.5W)^2}. \tag{14}$$

For the following roles C and D, the key angles are:

$$\begin{aligned}\delta_{\mathrm{C}}(t) &= 90^\circ - \gamma - \psi_O(t)\\ \delta_{\mathrm{D}}(t) &= \gamma - \psi_O(t),\end{aligned} \tag{15}$$

where $\delta_{\mathrm{C}}(t)$ and $\delta_{\mathrm{D}}(t)$ are the linking angles of role C and D. The reference position and heading of the tugboats then are expressed as:

$$\begin{aligned}\psi_{\mathrm{Cd}}(t) &= \alpha_{\mathrm{C}}(t) + \psi_O(t) - 90^\circ\\ x_{\mathrm{Cd}}(t) &= x_O(t) - L_O\cos\big(\delta_{\mathrm{C}}(t)\big) - L_{\mathrm{tow}}\cos\big(\psi_{\mathrm{Cd}}(t)\big)\\ y_{\mathrm{Cd}}(t) &= y_O(t) + L_O\sin\big(\delta_{\mathrm{C}}(t)\big) - L_{\mathrm{tow}}\sin\big(\psi_{\mathrm{Cd}}(t)\big),\end{aligned} \tag{16}$$

$$\begin{aligned}\psi_{\mathrm{Dd}}(t) &= \alpha_{\mathrm{D}}(t) + \psi_O(t)\\ x_{\mathrm{Dd}}(t) &= x_O(t) + L_O\sin\big(\delta_{\mathrm{D}}(t)\big) - L_{\mathrm{tow}}\cos\big(\psi_{\mathrm{Dd}}(t)\big)\\ y_{\mathrm{Dd}}(t) &= y_O(t) - L_O\cos\big(\delta_{\mathrm{D}}(t)\big) - L_{\mathrm{tow}}\sin\big(\psi_{\mathrm{Dd}}(t)\big).\end{aligned} \tag{17}$$

Besides, it is seen in Fig. 5 that the tug angle $\beta_I(t)$ in (9) can be solved by the towing angle, tugboat heading, and platform heading:

$$\begin{aligned}\beta_{\mathrm{A}}(t) &= \alpha_{\mathrm{A}}(t) + \psi_O(t) - 90^\circ - \psi_{\mathrm{A}}(t)\\ \beta_{\mathrm{B}}(t) &= \alpha_{\mathrm{B}}(t) + \psi_O(t) - \psi_{\mathrm{B}}(t)\\ \beta_{\mathrm{C}}(t) &= \alpha_{\mathrm{C}}(t) + \psi_O(t) - 90^\circ - \psi_{\mathrm{C}}(t)\\ \beta_{\mathrm{D}}(t) &= \alpha_{\mathrm{D}}(t) + \psi_O(t) - \psi_{\mathrm{D}}(t).\end{aligned} \tag{18}$$

B. Control Allocation Strategy

The control allocation system has two aims: (1) allocates the efforts to provide multiple control inputs $\boldsymbol{\tau}_{O_i}(t)$ to the platform; (2) calculates the thruster forces and moment of each tug $\boldsymbol{\tau}_{T_i}(t)$ to provide the corresponding towing force and track its reference trajectory. The control constraints of the towing system include the dynamics of the platform and tugs, the saturation of the towline and thrusters, and the restriction of the system configuration. Thus, considering the towing system is characterized by multiple control inputs and control constraints, the optimal control method is used to achieve control allocation and trajectory tracking.

The key to the problem then changes to the design of the cost function. For the offshore platform, the control objective is to track the waypoint, while its heading is not considered. So the cost function is designed as:

$$J_O(t) = w_{\mathrm{P}_O}\boldsymbol{e}_{\mathrm{P}_O}^{\mathrm{T}}(t)\boldsymbol{e}_{\mathrm{P}_O}(t) + w_{\mathrm{V}_O}\boldsymbol{V}_{O_{\mathrm{C}}}^{\mathrm{T}}(t)\boldsymbol{V}_{O_{\mathrm{C}}}(t), \tag{19}$$

where w_{P_O} and w_{V_O} are the weight coefficients of the platform (positive scalar); $\boldsymbol{e}_{\mathrm{P}_O}(t)\in\mathbb{R}^2$ and $\boldsymbol{V}_{O_{\mathrm{C}}}(t)\in\mathbb{R}^2$ are the position error and linear velocity of the platform, respectively, expressed as:

$$\begin{aligned}\boldsymbol{e}_{\mathrm{P}_O}(t) &= [x_{O_{\mathrm{C}}}(t) \;\; y_{O_{\mathrm{C}}}(t)]^{\mathrm{T}} - [x_{\mathrm{wp}}(j) \;\; y_{\mathrm{wp}}(j)]^{\mathrm{T}}\\ \boldsymbol{V}_{O_{\mathrm{C}}}(t) &= [u_{O_{\mathrm{C}}}(t) \;\; v_{O_{\mathrm{C}}}(t)]^{\mathrm{T}},\end{aligned} \tag{20}$$

where $x_{O_{\mathrm{C}}}(t)$, $y_{O_{\mathrm{C}}}(t)$ and $u_{O_{\mathrm{C}}}(t)$, $v_{O_{\mathrm{C}}}(t)$ are the calculated position and linear velocity of the platform.

The control objective of the tugboat is to track its reference trajectory, which contains the tug's position and heading, so the cost function is designed as:

$$J_i(t) = w_{\mathrm{P}_i}\boldsymbol{e}_{\eta_i}^{\mathrm{T}}(t)\boldsymbol{e}_{\eta_i}(t) + w_{\mathrm{V}_i}\boldsymbol{\nu}_{i_{\mathrm{C}}}^{\mathrm{T}}(t)\boldsymbol{\nu}_{i_{\mathrm{C}}}(t), \tag{21}$$

where w_{P_i} and w_{V_i} are the weight coefficients of the tugboat i (positive scalar); $\boldsymbol{\nu}_{i_{\mathrm{C}}}(t)\in\mathbb{R}^3$ is the calculated velocity vector; $\boldsymbol{e}_{\eta_i}(t)\in\mathbb{R}^3$ is the position and heading error of the tugboat i, expressed as:

$$\boldsymbol{e}_{\eta_i}(t) = \boldsymbol{\eta}_{i_{\mathrm{C}}}(t) - \boldsymbol{\eta}_{i_{\mathrm{d}}}(t), \tag{22}$$

where $\boldsymbol{\eta}_{i_{\mathrm{C}}}(t)\in\mathbb{R}^3$ and $\boldsymbol{\eta}_{i_{\mathrm{d}}}(t)\in\mathbb{R}^3$ are the calculated and reference position vector (position and heading) of the tugboat i, respectively.

The terms $x_{O_{\mathrm{C}}}(t)$, $y_{O_{\mathrm{C}}}(t)$, $u_{O_{\mathrm{C}}}(t)$ and $v_{O_{\mathrm{C}}}(t)$ in (20) are constrained by the platform dynamics, calculated by (1) – (6); the vectors $\boldsymbol{\nu}_{i_{\mathrm{C}}}(t)$ in (21) and $\boldsymbol{\eta}_{i_{\mathrm{C}}}(t)$ in (22) are constrained by the tugboat dynamics, calculated by the (1) and (7) – (9). The calculation of $\boldsymbol{\eta}_{i_{\mathrm{d}}}(t) = [x_{i\mathrm{d}}(t) \;\; y_{i\mathrm{d}}(t) \;\; \psi_{i\mathrm{d}}(t)]^{\mathrm{T}}$ is introduced in the previous section.

Then, the framework of the control allocation can be formulated as:

$$J^*(t) = \min_{\boldsymbol{\tau}_O(t),\boldsymbol{\tau}_i(t)}\Big(J_O(t) + \sum_{i=1}^{4} J_i(t)\Big), \tag{23}$$

Subject to $(i\in\{1,2,3,4\})$,

$$0^\circ \le \alpha_i(t) \le 90^\circ \tag{24}$$

$$0 \le F_i(t) \le F_{i\max} \tag{25}$$

$$-\boldsymbol{\tau}_{i\max} \le \boldsymbol{\tau}_i(t) \le \boldsymbol{\tau}_{i\max} \tag{26}$$

$$|\dot{\alpha}_i(t)| \le \bar{\alpha}_i \tag{27}$$

$$\big|\dot{F}_i(t)\big| \le \bar{F}_i \tag{28}$$

$$|\dot{\boldsymbol{\tau}}_i(t)| \le \bar{\boldsymbol{\tau}}_i, \tag{29}$$

where $F_{i\max}$ is the maximum value of towing force that the two towing lines withstand; $\boldsymbol{\tau}_{i\max}$ is the maximum value of the thruster forces and moment; $\bar{\alpha}_i$, $\bar{F}_i$ and $\bar{\boldsymbol{\tau}}_i$ are the maximum change rate value of the towing angles, the towing forces and the thruster forces and moment, respectively.

IV. SIMULATION EXPERIMENT

The simulated offshore platform is a virtual model based on [15] with the weight $m_O = 3.345$ kg and enlarged width and length $W = 1.2$ m, $L = 1.6$ m. The simulated tugboat is a virtual model based on [16] with the weight $m_O = 16.9$ kg and shrunk length $l_i = 0.6$ m. For the platform in the towing system, $L_{\mathrm{tow}} = 1.5$ m, $F_{i\max} = 0.3$ N, and $\bar{\alpha}_i = 5^\circ/\mathrm{s}$, $\bar{F}_i = 0.01$ N/s; for the each tugboat in the towing system, $\boldsymbol{\tau}_{i\max} = [2\ \mathrm{N} \;\; 2\ \mathrm{N} \;\; 1\ \mathrm{Nm}]^{\mathrm{T}}$ and $\bar{\boldsymbol{\tau}}_i = [1\ \mathrm{N/s} \;\; 1\ \mathrm{N/s} \;\; 0.5\ \mathrm{Nm/s}]^{\mathrm{T}}$.

The weight coefficients in cost function (19) and (21) are set as: $w_{\mathrm{P}_O} = 1$; $w_{\mathrm{V}_O} = 100$; $w_{\mathrm{P}_i} = 1$; $w_{\mathrm{V}_i} = 1$. We define two scenarios with the same control parameters and objectives to simulate the transportation process except that: the towing system in Scenario I applies the control scheme that the tag function $g(i)$ is constant for each tug i; while in Scenario II the system uses the proposed control scheme.

As shown in Fig. 6, four time-sampled states of the towing system illustrate the towing processes in two scenarios. From $\mathrm{t}_1 =$ 0s to $\mathrm{t}_2 = 135$ s, the platform and four tugs have the same trajectories which is the straight path, and tug 1 and 2 are the leader tugs, tug 3 and 4 are the follower tugs. After reaching the waypoint, the four tugboats keep their previous

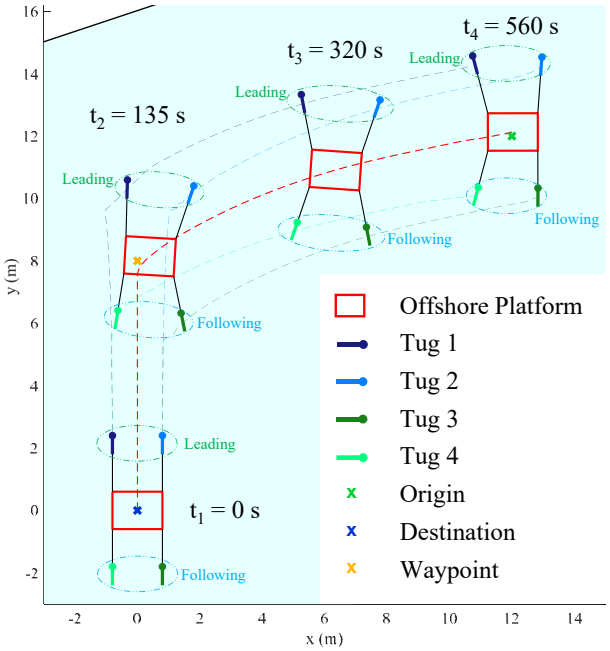

(a) Towing process in Scenario I

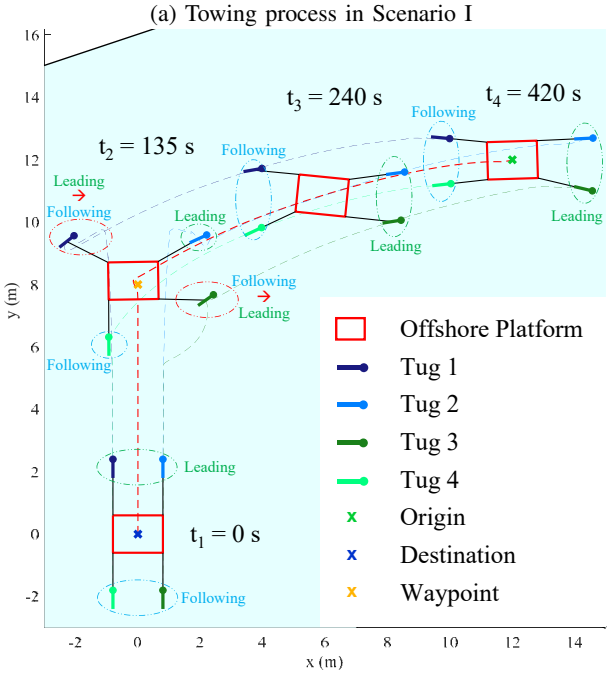

(b) Towing process in Scenario II

Fig. 6: Four time-sampled states of the towing system.

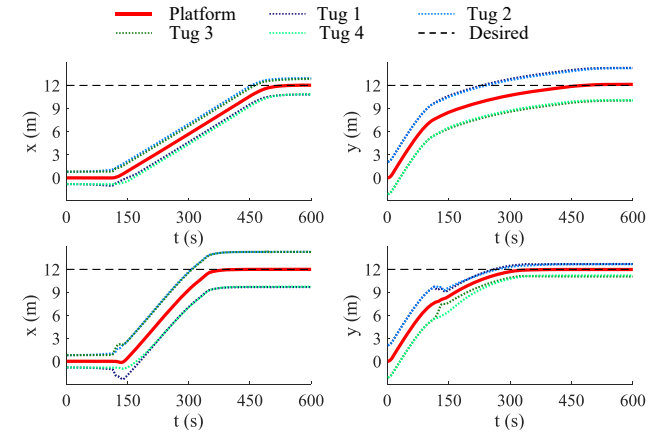

(a) Position of the platform and tugboats: the top two figures are Scenario I, the bottom two figures are Scenario II.

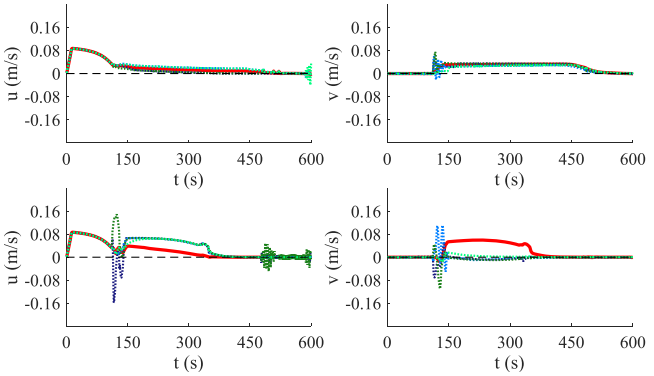

(b) Linear velocities of the platform and tugboats: the top two figures are Scenario I, the bottom two figures are Scenario II.

Fig. 7: Time-varying of the states for the platform and four tugboats in two scenarios.

configurations in Scenario I; while in Scenario II, because of the waypoint changing, tug 1 and tug 3 change their roles to become follower and leader tug, respectively.

From t_2 to t_3, the four tugboats of the towing system manipulate the platform with different configurations in two scenarios, and at time instant t_3 the configurations are different between Scenario I and II. t_4 is the settling time, at which the states of the ship satisfy the following conditions: *i*) the distance from the current position to the desired position is less than half length of the ship; *ii*) the surge and sway velocities are less than 0.01 m/s. It can be seen that the platform achieves its destination in both two scenarios, but the time cost in Scenario II is less.

The time-varying of the states for the platform and four tugboats in two scenarios are shown in Fig. 7. Fig. 7 (a) is the changes of position. It can be seen that the coordinates of the platform reach the desired values in two scenarios, but Scenario II reaches the values first. In addition, the positions of four tugs in Scenario II have big changes around 135s, which is the time instant of waypoint changing. Fig. 7 (b) is the changes of linear velocity. The velocities of the platform reach their desired values in two scenarios, and after the waypoint changing (135 s), the velocities of four tugs also reflect big changes in Scenario II, which leads to the increase of the platform velocities. The above position and velocity changes explain the reason for the less time cost of the towing process in Scenario II.

The values of the towing angles and forces are seen in Fig. 8, which satisfy the saturation constraints. Due to the tug role switching in Scenario II, the magnitude changes of the towing angles in this scenario are shown greater than those in Scenario I. As for the towing forces, except for F_4 that has no changes in both scenarios, the rate changes of the other three forces in Scenario II are higher than those

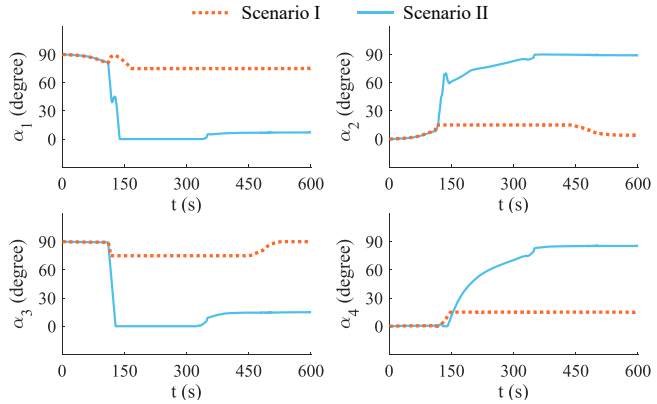

(a) Value of the four towing angles

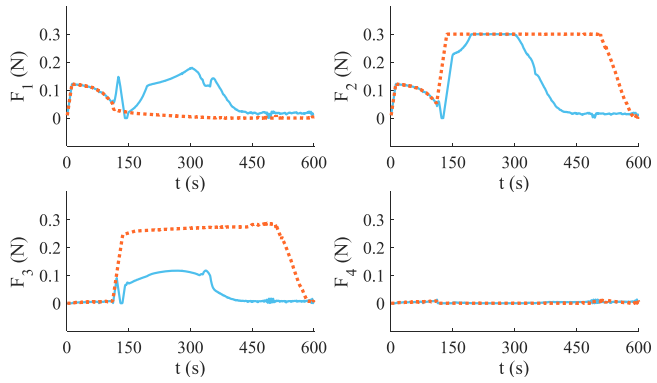

(b) Value of the four towing forces

Fig. 8: Time-varying of the control inputs for the platform in two scenarios.

in Scenario I. This explains the bigger changes of the linear velocities in Scenario II. It is noticed that the magnitudes of these forces are small because the weight of the tugboat is 5 times of the platform, there is no need much forces to manipulate the platform. It can also be seen from Fig. 8 that there are not many fluctuations in towing angles and forces, even in switching between leaders and followers.

V. CONCLUSIONS AND FUTURE RESEARCH

This paper proposed a dynamic coordination control scheme for the transportation of an offshore platform with a physically connected multi-vessel towing system. The dynamic coordination decision mechanism and the control allocation strategy formed the core of the proposed scheme. The decision mechanism was designed through the relations of current platform states and next waypoint position, and four role combinations were defined for dealing with different scenarios. Based on the assigned tug roles, the corresponding real-time reference trajectory of the tugboats was calculated for motion coupling between the platform and tugboats. The control allocation strategy was developed by the optimization method to track the dynamic reference trajectory of tugboats considering multiple constraints. A simulation experiment indicated that the proposed control scheme can enhance the maneuverability of the physically connected multi-vessel towing system and increase the efficiency of offshore platform transportation.

Future research will focus on dealing with environmental disturbances and designing a distributed control architecture for the offshore platform towing system.

ACKNOWLEDGMENT

This research is supported by the China Scholarship Council under Grant 201806950080, the Researchlab Autonomous Shipping (RAS) of Delft University of Technology, and the INTERREG North Sea Region Grant “AVATAR” funded by the European Regional Development Fund.

REFERENCES

[1] B. J. Leira, “Multi-purpose offshore-platforms: Past, present and future research and developments,” in *Proceedings of the ASME 36th International Conference on Ocean, Offshore and Arctic Engineering-Volume 3A: Structures, Safety and Reliability*, Trondheim, Norway, 2017, pp. 1–11.

[2] Z. Du, V. Reppa, and R. R. Negenborn, “Cooperative control of autonomous tugs for ship towing,” *IFAC-PapersOnLine*, vol. 53, no. 2, pp. 14 470–14 475, 2020.

[3] E. Tuci, M. H. M. Alkilabi, and O. Akanyeti, “Cooperative object transport in multi-robot systems: A review of the state-of-the-art,” *Frontiers in Robotics and AI*, vol. 5, pp. 1–15, 2018.

[4] M. G. Feemster and J. M. Esposito, “Comprehensive framework for tracking control and thrust allocation for a highly overactuated autonomous surface vessel,” *Journal of Field Robotics*, vol. 28, no. 1, pp. 80–100, 2010.

[5] V. P. Bui, H. Kawai, Y. B. Kim, and K. S. Lee, “A ship berthing system design with four tug boats,” *Journal of Mechanical Science and Technology*, vol. 25, no. 5, pp. 1257–1264, 2011.

[6] L. Chen, H. Hopman, and R. R. Negenborn, “Distributed model predictive control for cooperative floating object transport with multi-vessel systems,” *Ocean Engineering*, vol. 191, p. 106515, 2019.

[7] Y. Zheng, J. Tao, Q. Sun, H. Sun, M. Sun, and Z. Chen, “An intelligent course keeping active disturbance rejection controller based on double deep q-network for towing system of unpowered cylindrical drilling platform,” *International Journal of Robust and Nonlinear Control*, vol. 31, no. 17, pp. 8463–8480, aug 2021.

[8] H. Hajieghrary, D. Kularatne, and M. A. Hsieh, “Differential geometric approach to trajectory planning: Cooperative transport by a team of autonomous marine vehicles,” in *Proceedings of the 2018 Annual American Control Conference (ACC)*, Milwaukee, WI, USA, 2018, pp. 858–863.

[9] G. Xia, C. Sun, B. Zhao, X. Sun, and X. Xia, “Robust cooperative trajectory tracking control for an unactuated floating object with multiple vessels system,” *ISA Transactions*, pp. 1–9, 2021.

[10] Z. Du, R. R. Negenborn, and V. Reppa, “Cooperative multi-agent control for autonomous ship towing under environmental disturbances,” *IEEE/CAA Journal of Automatica Sinica*, vol. 8, no. 8, pp. 1365–1379, 2021.

[11] Z. Du, R. R. Negenborn, and V. Reppa, “MPC-based colregs compliant collision avoidance for a multi-vessel ship-towing system,” in *Proceedings of the European Control Conference*, Rotterdam, the Netherlands, 2021, pp. 1–6.

[12] Z. Du, R. R. Negenborn, and V. Reppa, “Multi-vessel cooperative speed regulation for ship manipulation in towing scenarios,” *IFAC-PapersOnLine*, vol. 54, no. 16, pp. 384–389, 2021.

[13] T. I. Fossen, *Handbook of Marine Craft Hydrodynamics and Motion Control*. Chichester, West Sussex, UK: John Wiley & Sons, 2011.

[14] H. Hensen, *Tug Use in Port: A Practical Guide*. London, UK: Nautical Institute, 2003.

[15] L. Chen, Y. Huang, H. Zheng, H. Hopman, and R. Negenborn, “Cooperative multi-vessel systems in urban waterway networks,” *IEEE Transactions on Intelligent Transportation Systems*, vol. 21, no. 8, pp. 3294–3307, 2020.

[16] A. Haseltalab and R. R. Negenborn, “Model predictive maneuvering control and energy management for all-electric autonomous ships,” *Applied Energy*, vol. 251, no. 113308, pp. 1–27, 2019.